RANDOM FLUTTER OF MULTI-STABLE AIRFOILS EXCITED PARAMETRICALLY IN STEADY FLOWS

Y. Hao

College of Civil Engineering & Mechanics
Yanshan University
Qinhuangdao, China

Z. Q. Wu*

School of Mechanical Engineering
Tianjin University
Tianjin, China

ABSTRACT

In this article, random flutter of multi-stable airfoils in steady flow is investigated by means of the analytical method for stochastic P-bifurcation, where the effect of the stochastic disturbance in the generalized flow speed on the airfoils is considered. The results show that under constant stochastic disturbance intensity, the coherence resonance could be induced by the variation of generalized flow speed. In addition, if the generalized flow speed keeps unchanged and its stochastic disturbance is sufficiently large, the response of the system will tend to be a stable equilibrium. It indicates that the parametric stochastic disturbance is effective to maintain system stability. Moreover, it is shown in this paper that the analytical method for stochastic P-bifurcation can be extended to study stochastic P-bifurcations in other high-dimensional systems.

Keywords: Stochastic P-bifurcation, Stochastic parametric excitation, Random flutter.

1. INTRODUCTION

Limit cycle flutter is a typical kind of nonlinear dynamics behavior of airfoil dynamics, which usually poses a direct threat to flight safety. It is known that limit cycle generated by supercritical Hopf bifurcation is the soft-destabilization whereas the limit cycle generated by sub-critical Hopf bifurcation with the saddle-note bifurcation is hard-destabilization. Researches have been found that utilize the random process to simulate turbulence around the airfoils. Significant results are discovered that are unable to be obtained under the deterministic analysis methods. This motivates the application of random process theories to study the airfoil dynamics under stochastic external disturbance in this paper.

Rich results can be found when considering the stochastic influence for soft destabilization. Poirel studied the perturbation of turbulent flow in the 90s with the turbulence modeled as a random process. Based upon the research from Ref. [1], Poirel [2] studied the effect of longitudinal atmospheric turbulence on the dynamics of an airfoil with a hardening cubic structural nonlinearity for pitch and a continuous stochastic approach is required for the turbulence model. The power spectral density (PSD) curves of the pitch angle were analyzed for different flow speed and the influence of structural parameters on flutter speed was also discussed. In 1999, the same research group published an overview about structural and aero-elastic nonlinearities [3]. Then Poirel [4, 5] conducted further research which considered the turbulence on both longitudinal and vertical directions. It is shown that turbulent, due to its longitudinal component, destabilizing the aero-elastic system by advancing the flutter point and decreasing the damping. It was found by Poirel that depending on the variance of turbulence excitation and the nonlinear cubic stiffness value, the marginal probability density functions (PDFs) of pitch angle exhibit uni-, bi- or double bi-modality. Since 2007, Poirel [6] started to focus on the stochastic bifurcation of airfoil flutter dynamics. In recent years, extensive experimental studies [7-10] were published. Poirel and colleague conducted a series of wind tunnel test of NACA0012 airfoil and analyzed the limit cycle behavior of the aero-elastic system at low-to-moderate Reynolds number. The small and large amplitude limit

* Corresponding author (zhiqwu@tju.edu.cn)

DOI : 10.1017/jmech.2018.19
Copyright © 2018 The Society of Theoretical and Applied Mechanics
https://doi.org/10.1017/jmech.2018.19 Published online by Cambridge University Press

cycle oscillation were reported at [9] with different initial conditions. Zhao *et al*. [11, 12] studied the two degree-of-freedom (DOF) airfoil model with Hopf bifurcation. The work analyzed the joint PDF, marginal PDF and greatest Lyapunov exponent. Meanwhile, Yang, Zhao [13] and Berggren [14] also observed the phenomenon of limit cycle oscillations (LCO) from experiments. Other experimental study of LCO of airfoil can be found from the works by Chassasing [15] and Dowell E. H. [16].

In addition, some scholars introduced higher-order nonlinearity to investigate the multi-stable characteristics (hard-destabilization) of airfoil flutter. Christiansen [17] described the effects of random external excitations on the flutter of a high aspect ratio wing. In order to study the significance of random airflow fluctuations with presence of subcritical flutter transition, Ref. [17] considered two nonlinear models: an extended normal-form model and a nonlinear version of a 2 DOF structural models. Both models yield the same discovery. In Ref. [17], the variation of the regularity parameter with respect to noise level and the flow speed for the nonlinear 2 DOF structural model were discussed, and the subcritical Hopf bifurcation and the saddle-node bifurcation were observed. At the interval between these two bifurcations, the unstable limit cycle represents a separatrix between the equilibrium state and the flutter state. Reference [18] introduces a methodology for the reliability-based design optimization of systems with nonlinear aeroelastic constraints. The proposed approach was applied to the generation of flutter and subcritical LCO boundary finding of a 2 DOF airfoil with a fifth order nonlinear stiffness. Moreover, Dribush C. [19, 20] also considered the quantic nonlinearity stiffness when studying the stability boundary of aero-elastic problems. Meantime Dimitriadis [21] reported the local bifurcation found from experimental studies, the existence of stochastic external excitation and aerodynamic load lead to the discovery of subcritical Hopf bifurcation and secondary bifurcation. This implies the system has multiple steady states.

Although some results for stochastic flutter of the high dimensional nonlinear airfoil were obtained via numerical simulation or experimental methods, few publications were found using analytic method to study such problems. This paper studies the flutter of a typical 2 DOF airfoil model with the stochastic disturbance on flow speed. The modified averaging method is applied herein to reduce the system dimension. The critical parametric conditions for stochastic P-bifurcation of airfoil are deduced by means of stochastic averaging and singularity theory. The influences of stochastic disturbance and flow speed on system response and the flutter behavior are discussed.

2. DYNAMICAL MODEL OF AIRFOIL FLUTTER

The airfoil is modelled as a rigid flat plate, with degrees of freedom in pitch and plunge. A quantic representation of the torsional spring is considered, this is the source of nonlinearity considered in this paper. The structural equations include the nonlinearity and stochastic disturbance are as follows [22]

$$\begin{cases} M\ddot{h} + S\ddot{\alpha} - c_1\dot{h} + K_h h = A \\ S\ddot{h} + J_E\ddot{\alpha} - c_2\dot{\alpha} + K_\alpha \alpha = B \end{cases} \tag{1}$$

where h and α are the airfoil motion in plunge and pitch directions, c_1 and c_2 represent the damping coefficient at h and α, respectively. The stiffness of α is $K_\alpha = k_{\alpha 1} + k_{\alpha 3}\alpha^2 + k_{\alpha 5}\alpha^4$, here, $k_{\alpha 1}$ is the linear stiffness coefficient, $k_{\alpha 3}$ and $k_{\alpha 5}$ are the nonlinear stiffness coefficients [18-20]. The purpose of introducing the quantic representation of the torsional spring is to study the behavior of bi-stable with equilibrium and limit cycle subjected to parametric stochastic disturbance. The structure parameters are given as,

$$\begin{cases} M = 1, \quad S = 0.25, \quad K_h = 0.2, \quad c_1 = 0.1 \\ J_E = 0.25, \quad c_2 = 0.1, \quad K_\alpha = k_{\alpha 1} + k_{\alpha 3}\alpha^2 + k_{\alpha 5}\alpha^4 \\ A = -0.1(Q + \xi(t))\alpha \\ B = 0.04(Q + \xi(t))\alpha \\ k_{\alpha 3} = -0.0198, \quad k_{\alpha 5} = 0.0108 \end{cases}$$

where Q is generalized flow speed, the stochastic disturbance $\xi(t)$ is considered in Q, we assumed that $Q + \xi(t)$, and $\xi(t)$ is the Gaussian white noise with zero-mean and intensity D.

3. POWER DENSITY DISTRIBUTION OF AEROELASTIC MODAL AMPLITUDE

In order to solve Eq. (1), we apply the modified averaging method [23]. Let $\mathbf{x} = \begin{pmatrix} x_1 \\ x_2 \\ x_3 \\ x_4 \end{pmatrix} = \begin{pmatrix} \alpha \\ \dot{\alpha} \\ h \\ \dot{h} \end{pmatrix}$, Eq. (1) can be expressed as

$$\dot{\mathbf{x}} = F(x, Q, t) \tag{2}$$

Let Q be the bifurcation parameter, in addition, we assume Q_0 is the critical bifurcation point of deterministic system. The Jacobian matrix at Q_0 can be obtained for the deterministic system, whose eigenvalues include a pair of pure imaginary roots and other roots with negative real parts. Let $Q = Q_0 + u$, we assume the random disturbance $\xi(t)$ is small and introduce a small parameter μ, then, the perturbation near the Hopf bifurcation point is $u = \mu + \xi(t)$. Hence, the Jacobian matrix with perturbation can be rewritten as

$$\mathbf{A}(u) = \mathbf{A}(0, u, 0) = \left.\frac{\partial F}{\partial x}\right|_{\substack{x=0 \\ Q=Q_0+u \\ t=0}} \tag{3}$$

Expanding Eq. (3) at $u = 0$ yields, $\mathbf{A}(u) = \mathrm{A}_0 + D\mathbf{A}(u)|_{u=0}\, u = \mathbf{A}_0 + \mathbf{A}_1 u$, Hence, Eq. (2) can be rewritten

https://doi.org/10.1017/jmech.2018.19 Published online by Cambridge University Press

as

$$\dot{\mathbf{x}} = (\mathbf{A}_0 + \mathbf{A}_1 u)\mathbf{x} + [F(x,Q,t) - (\mathbf{A}_0 + \mathbf{A}_1 u)\mathbf{x}] = \mathbf{A}_0\mathbf{x} + \mathbf{F}_a(x,u) \tag{4}$$

where, $\mathbf{F}_a(x,u)$ is the quadratic polynomials, and $\dot{\mathbf{x}} = \mathbf{A}_0\mathbf{x}$ is the derived system. Let us assume the solution of the derived system as

$$\mathbf{x} = \mathbf{G}(t)\mathbf{b} \tag{5}$$

where $\mathbf{G}(t) = \mathbf{TE}(t)$ is the fundamental matrix of Eq. (2), $\mathbf{E}(t) = diag(e^{\lambda_1 t}, e^{\lambda_2 t}, e^{\lambda_3 t}, e^{\lambda_4 t})$, $\mathbf{T} = (\varphi_1, \varphi_2, \varphi_3, \varphi_4)$, and $\mathbf{b}$ is a function of t, λ_j is the eigenvalue of Jacobian matrix, λ_1, λ_2 is the pair of pure imaginary, and the other two (λ_3, λ_4) have negative real parts, φ_j is the eigenvector corresponds to each eigenvalue. Due to the variation of parameters, Eq. (5) also can be used to represent the solution of the nonlinear system with the form $\dot{\mathbf{x}} = \mathbf{A}_0\mathbf{x} + \mathbf{F}_a(x,u)$. Substituting Eq. (5) into Eq. (4), we have

$$\dot{\mathbf{b}} = \mathbf{G}^*(t)\mathbf{F}_a(x,u)|_{\mathbf{x}=\mathbf{G}(t)\mathbf{b}} = \mathbf{H}(b,u,t) = \begin{pmatrix} \mathbf{H}_1 \\ \mathbf{H}_2 \\ \mathbf{H}_3 \\ \mathbf{H}_4 \end{pmatrix} \tag{6}$$

where $\mathbf{G}^*(t)$ is the inverse of fundamental matrix $\mathbf{G}(t)$. In order to derive the solution in a more familiarized format, we assume the solution of Eq. (6) has the form:

$$\begin{cases} b_1 = re^{(i\theta)} \\ b_2 = re^{(-i\theta)} \\ b_3 = b_3 \\ b_4 = b_4 \end{cases} \tag{7}$$

Since we are only interested in the long term behavior of the system, when t approaches infinity, $b_3 = b_4 = 0$. Therefore, we obtain the normal equation by substituting Eq. (7) into Eq. (6):

$$\begin{cases} \dot{r} = [\mathbf{H}_1 \cos\theta + \mathbf{H}_2 \sin\theta] = \Phi(r,\theta,\mu) \\ \dot{\theta} = [-\mathbf{H}_1 \sin\theta + \mathbf{H}_2 \cos\theta]/r_j = \Phi^*(r,\theta,\mu) \end{cases} \tag{8}$$

where,

$$\begin{aligned}\Phi(r,\theta,\mu) = {} & [-23.1688 - 29.6593\cos(1.5244t - 2\theta) - 18.9576\sin(1.5244t - 2\theta) - 6.2368\cos(3.0488t - 4\theta) \\ & -13.2086\sin(3.0488t - 4\theta) - 2.5597\sin(4.5733t - 6\theta) + 0.2729\cos(4.5733t - 6\theta)]k_{\alpha 5}r^5 \\ & +[-6.3246 - 5.2253\sin(1.5244t - 2\theta) - 6.9269\cos(1.5244t - 2\theta) - 2.2363\sin(3.0488t - 4\theta) \\ & -0.6977\cos(3.0488t - 4\theta)]k_{\alpha 3}r^3 + [0.1402 + 0.1341\sin(1.5244t - 2\theta) \\ & +0.0948\cos(1.5244t - 2\theta)]r(\mu + \xi(t))\end{aligned}$$

$$\begin{aligned}\Phi^*(r,\theta,\mu) = {} & [11.2231 - 3.9404\sin(1.5244t - 2\theta) + 20.0513\cos(1.5244t - 2\theta) - 1.4296\sin(3.0488t - 4\theta) \\ & +11.3654\cos(3.0488t - 4\theta) + 0.2729\sin(4.5733t - 6\theta) - 2.5597\cos(4.5733t - 6\theta)]k_{\alpha 5}r^4 \\ & +[3.0639 - 2.2460\sin(1.5244t - 2\theta) + 5.4243\cos(1.5244t - 2\theta) - 0.6977\sin(3.0488t - 4\theta) \\ & +2.2363\cos(3.0488t - 4\theta)]k_{\alpha 3}r^2 + [-0.0853 + 0.0948\sin(1.5244t - 2\theta) \\ & -0.1340\cos(1.5244t - 2\theta)](\mu + \xi(t))\end{aligned}$$

The normal equation is about r and θ, r represents the aero-elastic modal amplitude. By substituting $\boldsymbol{G(t)}$ and $\boldsymbol{b}$ into $\mathbf{x} = \mathbf{G}(t)\mathbf{b}$, we have the expression of $\mathbf{x}$, where $\varphi = 0.7622t + \theta$,

$$\mathbf{x} = \begin{pmatrix} \alpha \\ \dot{\alpha} \\ h \\ \dot{h} \end{pmatrix} = \begin{pmatrix} -2.0529r\cos(\varphi) - 0.4254r\sin(\varphi) \\ -0.3242r\cos(\varphi) + 1.5648r\sin(\varphi) \\ -5.6080r\cos(\varphi) - 0.0384r\sin(\varphi) \\ -0.0292r\cos(\varphi) + 4.2745r\sin(\varphi) \end{pmatrix} \tag{9}$$

The stochastic average and deterministic average could be utilized for the normal equation Eq. (8), and we obtain the following stochastic equations for the aero-elastic modal amplitude r and θ,

$$\begin{aligned} \mathrm{d}r &= (-23.1668k_{\alpha 5}r^5 - 6.3246k_{\alpha 3}r^3 + 0.1402r\mu + 0.0062Dr)\mathrm{d}t + \sqrt{0.0663r^2 D}\,\mathrm{d}W_1(t) \\ \mathrm{d}\theta &= (11.2230k_{\alpha 5}r^4 + 3.0639k_{\alpha 3}r^2 - 0.08531\mu)\mathrm{d}t + \sqrt{0.0415D}\,\mathrm{d}W_2(t) \end{aligned} \tag{10}$$

where D is the intensity of stochastic disturbance $\xi(t)$, $W_1(t)$ and $W_2(t)$ are two independent Winner processes. For $D \neq 0$, the probability density function $p(r,t)$ of the instantaneous aero-elastic modal amplitude r satisfies the FPK equation,

https://doi.org/10.1017/jmech.2018.19 Published online by Cambridge University Press

$$\frac{\partial p(r,t)}{\partial t}=-\frac{\partial}{\partial r}[(-23.1668k_{\alpha 5}r^5-6.3246k_{\alpha 3}r^3+0.1402r\mu+0.0062Dr)p(r,t)]+\frac{1}{2}\frac{\partial^2}{\partial r^2}[0.0663r^2Dp(r,t)] \tag{11}$$

The stationary solution of FPK equation is,

$$p_s(r)=\kappa\frac{15.0854r^{\frac{4.2315\mu}{D}-1.8131}\exp\left(\frac{-1.8857r^4+1.8857r^2}{D}\right)}{D} \tag{12}$$

with κ the normalization constant. The relation between $\alpha, \dot{\alpha}, h, \dot{h}$ and r, θ can be found in Eq. (9). Thus, we have the analytical expression of $p_s(r_\alpha)$ and $p_s(r_h)$, which are the PDFs of pitch angle and plunge displacement,

$$p_s(r_\alpha)=\kappa_1\frac{15.0854(0.4770r_\alpha)^{\frac{4.2315\mu}{D}-1.8131}\exp\left(\frac{-0.0976r_\alpha^4+0.4290r_\alpha^2}{D}\right)}{D} \tag{13}$$

$$p_s(r_h)=\kappa_2\frac{15.0854(0.1783r_h)^{\frac{4.2315\mu}{D}-1.8131}\exp\left(\frac{-0.0019r_h^4+0.0600r_h^2}{D}\right)}{D} \tag{14}$$

Moreover, θ can be regarded as a random variable with the uniform distribution. Substituting Eqs. (13), (14) into (9), we also have the expressions of $p_s(\alpha,\dot{\alpha})$ and $p_s(h,\dot{h})$:

$$p_s(\alpha,\dot{\alpha})=\frac{1}{2\pi}\frac{1}{D}\left\{15.0854(0.4770r_\alpha)^{\frac{4.2315\mu}{D}-1.8131}\exp\left(\frac{-0.0976r_\alpha^4+0.4290r_\alpha^2}{D}\right)\right\}\left|\frac{\partial(r_\alpha,\theta)}{\partial(\alpha,\dot{\alpha})}\right| \tag{15}$$

$$p_s(h,\dot{h})=\frac{1}{2\pi}\frac{1}{D}\left\{15.0854(0.1783r_h)^{\frac{4.2315\mu}{D}-1.8131}\exp\left(\frac{-0.0019r_h^4+0.0600r_h^2}{D}\right)\right\}\left|\frac{\partial(r_h,\theta)}{\partial(h,\dot{h})}\right| \tag{16}$$

4. BIFURCATION ANALYSIS OF DETERMINISTIC SYSTEM

The bifurcation of deterministic system can be characterized by Fig. 1. In Fig. 1, the horizontal axis represents the perturbation close to the bifurcation point Q_0 and longitudinal axis represents the amplitude of pitch angle and plunge displacement. The dotted lines are the unstable limit cycle while solid line is the equilibrium and stable limit cycles. It can be seen from Fig. 1 that bi-stable state exists in the system. Note Fig. 1 shows the results solved from the first order approximation via the modified averaging method and the averaging method respectively (please refer to the two subplots of Fig. 1). As mentioned previously, it is the high order nonlinearity at $K_\alpha = k_{\alpha 1} + k_{\alpha 3}\alpha^2 + k_{\alpha 5}\alpha^4$ that causes the second bifurcation and bi-stable steady state. Blue stars shown in Fig. 1 are the numerical results by adopting Rung-Kutta fourth-order algorithm. Good agreements between numerical and analytical methods can be discovered in Fig. 1, which validates the proposed solving approach and dimension reduction scheme.

The main parameter involves in airfoil flutter is the critical generalized flow speed, which is the critical value of Q. In Fig. 1, $\mu = 0$ corresponds to $Q_H = 11.84493764$ is the Hopf bifurcation point, which is known as the first critical speed or linear critical generalized flow speed. The nonlinear critical speed arrives when $\mu = -0.1114082323$, which corresponds to $Q_A = 11.73085532$, where the pitch-fork bifurcation occurs. From Fig. 1 it can be seen that the nonlinear critical speed is less than its linear counterpart. Nevertheless, large amplitude vibration occurs if the generalized flow speed is greater than the nonlinear critical speed.

5. BIFURCATION ANALYSIS OF STOCHASTIC SYSTEM

The bifurcation equation [24, 25] of the 2 DOF airfoil model is,

$$g(r)=R(r,D,\mu)\exp(Q(r,D,\mu))-p_s(r)=0 \tag{17}$$

here:

$$R(r,D,\mu)=\frac{15.0854r^{\frac{4.2315\mu}{D}-1.8131}}{D}$$

$$Q(r,D,\mu)=\frac{-1.8857r^4+1.8857r^2}{D}$$

According to Wu [24, 25], the variation number of peaks of the PDF is the transition set H, here

$$H=\{p_s=R(r,D,\mu)\exp(Q(r,D,\mu)),\ R'+RQ'=0,$$
$$R''+2R'Q'+RQ''+RQ'^2=0\}$$

https://doi.org/10.1017/jmech.2018.19 Published online by Cambridge University Press

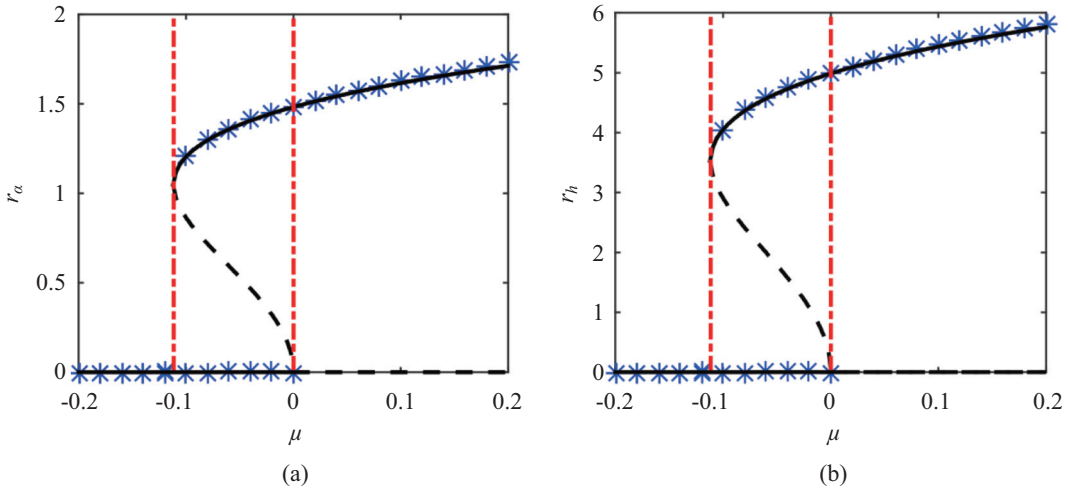


Fig. 1 Bifurcation diagram of deterministic system.

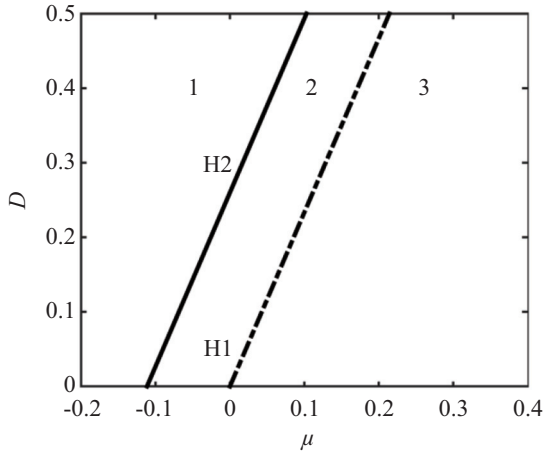


Fig. 2 The critical condition of the P-bifurcation (Transition sets).

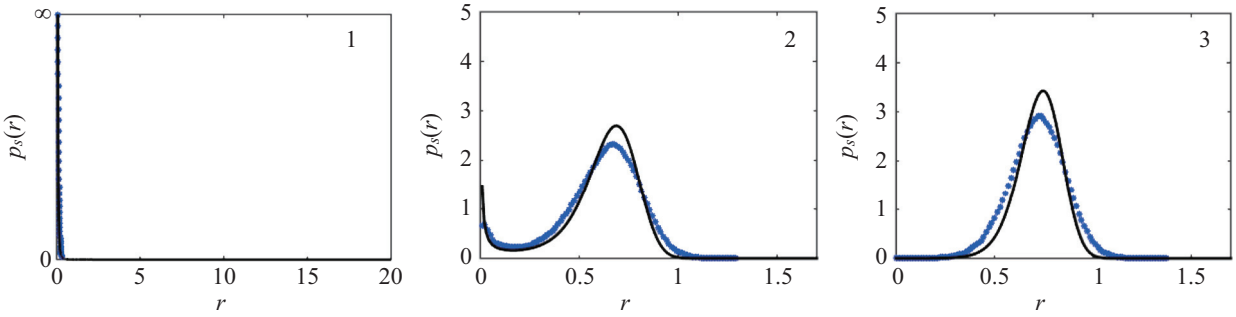


Fig. 3 PDF curves of modal amplitude r under different regions in parameter plane (shown in Fig. 2).

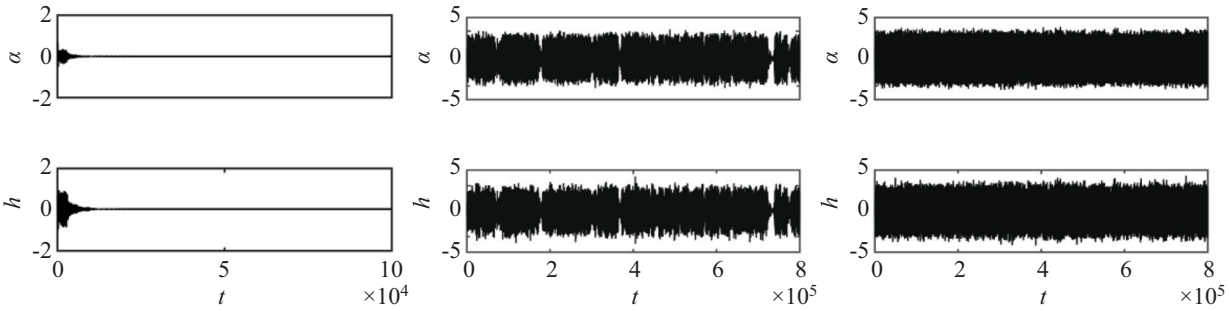
The analytical expressions of the critical parameter that enables the occurrence of stochastic P-bifurcation are,

$$\text{H1}: \mu = 0.4285D - 0.1114$$
$$\text{H2}: \mu = 0.4285D \tag{18}$$

The intersections of H1, H2 and D = 0 correspond to the linear and nonlinear critical generalized flow speed (Q_H = 11.84493764, Q_A = 11.73085532) in Fig. 1. These two straight lines divide the parameter space where D > 0 into three domains as shown in Fig. 2. These three regions correspond to three different kinds of steady state PDFs as can be found in Fig. 3.

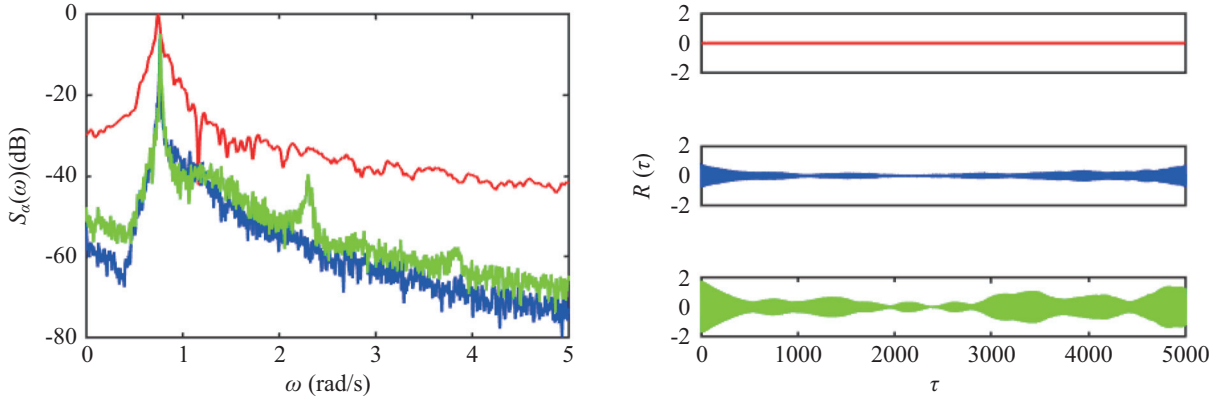
In Fig. 3 the black solid line represents the theoretical prediction from the stochastic averaging method, blue

https://doi.org/10.1017/jmech.2018.19 Published online by Cambridge University Press



(a) μ = -0.15, D = 0.1 (b) μ = 0.02, D = 0.1 (c) μ = 0.6, D = 0.1

Fig. 4 Typical time response under different regions of the parameter plane (shown in Fig. 2).



(a) (b)

Fig. 5 Coherence resonance with constant disturbance intensity and varying flow speed (D = 0.1, μ = -0.15, 0.02, 0.6).

stars represent the Monte Carlo simulation results. The Rung-Kutta fourth-order algorithm is adopted to acquire the time history of each sample. The integration time is selected long enough, after 10000 iterations, the simulation run until steady state is reached. We ran the Monte Carlo simulation with sample number set as 10^6.

The PDF of aero-elastic modal amplitude r obtained from region 1 (in Fig. 2) of the (D, μ) parameter plane is shown in Fig. 3(a). No large amplitude vibration is observed at this region. The probability of large amplitude vibration under this circumstance is almost zero, and the time responses of α, h shown in Fig. 4(a) also verify the probabilistic distribution.

An obvious peak will occur in the PDF curve when the parameter set is chosen in region 2 (in Fig. 2) of the (D, μ) plane, as shown in Fig. 3(b). Large amplitude vibration can be found but small vibration still exists. System response stays between the two steady states. Time domain results of α, h are shown in Fig. 4(b).

Further increases in airspeed Q cause the PDF curves reduce to only one peak, large amplitude vibration dominates the dynamics in this case, as shown in Fig. 3(c) and Fig. 4(c), the system behaves like a diffused limit cycle.

Based on the information shown in Figs. 3 and 4, it can be found that the stochastic P-bifurcation will happens with the increasing of the Q. The stochastic P-bifurcation is also associated with the PDF curves of r starts to show an obvious peak. The transition of PDF shape is accompanied by the vibration pattern change at steady state responses. When (D, μ) falls into region 3 (in Fig. 2), the system depict the LCO motion similar as in the deterministic case. With the increasing of D (intensity of stochastic disturbance $\xi(t)$), the parameter set will cross the hysteresis set H1 or even the H2 and reach to region 1 (in Fig. 2), this crossing is the occurrence of stochastic P-bifurcation. The crossing at this direction is associated with the decreasing of vibration amplitude until the motion decays to equilibrium. To this extend, the stochastic disturbance is beneficial to system response by suppressing the large deformation.

6. COHERENT RESONANCE AND THE INFLUENCE OF SYSTEM PARAMETERS

In this section, we first discuss the coherent resonance induced by flow speed changing under constant stochastic disturbance intensity. Figure 5 gives the power density spectrum (PDS) curves and the correlation function of pitch angle with μ = -0.15 (red), 0.02 (blue) and 0.6 (green).

When the Q increases, the energy distribution bears

https://doi.org/10.1017/jmech.2018.19 Published online by Cambridge University Press

the following transfer process: wide spectrum narrows down rapidly and then turns wider gradually with the maximum value stays at the natural frequency. Similar phenomenon was discovered when Zakharova [26] studies the P-bifurcation of bi-stable van der Pol equation under additive stochastic excitation. However, what differs the phenomenon discover herein is that the random excitation is multiplicative. The underlying physical mechanism of this changing behavior under multiplicative noise would be detailed in future publications.

7. CONCLUSIONING REMARKS

In this article, the multi-stable airfoil in steady flow with stochastic disturbance is studied through a nonlinear two-degree-of-freedom dynamical system. Stochastic parametric excitation and stochastic P-bifurcation are investigated. Dimension reduction is conducted by the modified averaging method, and the steady state probability density distribution (PDF) for pitch angle and plunge displacement are obtained by using of stochastic averaging method. The critical conditions of stochastic P-bifurcation are identified by means of the singularity analysis theory. Three different patterns PDF curves and time history curves of the steady-state responses are discovered via the analytical approach.

Moreover, the analysis results show that the critical generalized flow speed (Q_H and Q_A) are delayed with the increasing of the stochastic parametric excitation intensity. In the linear unstable region, the increasing of the stochastic parametric excitation intensity could inhibit limit cycle oscillation (LCO). It is found that the power spectrum density (PSD) of the pitch angle exhibits maximum value at the corresponding natural frequency. With the increasing of Q, LCO occurs in the system.

ACKNOWLEDGEMENTS

This research is supported by the following projects: National Science Foundation of China (No. 11372211, 11672349, 11172198); Science and Technology research Project of Colleges and universities in Hebei province, China (No.2016045); The Doctoral Starting up Foundation of Yanshan University, China (B938); Science and Technology of Qinhuangdao, China (No.2015A248).

NOMENCLATURE

α, h	airfoil motion in plunge and heave directions
K_α	stiffness coefficient at α
$k_{\alpha 1}$	linear stiffness coefficient
$k_{\alpha 3}$, $k_{\alpha 5}$	nonlinear stiffness coefficients
K_h	stiffness coefficient at h
c_1, c_2	damping coefficient at h and α
Q	generalized flow speed
$\xi(t)$	stochastic disturbance in Q
D	intensity of the stochastic disturbance
μ	the perturbation nearby the Hopf bifurcation point
r	aero-elastic modal amplitude
r_α	amplitude of α
r_h	amplitude of h
Q_H	linear critical generalized flow speed
Q_A	nonlinear critical generalized flow speed

REFERENCES

1. Price, S. J. and Alighanbari, H., "The Aeroelastic Response of a Two-Dimensional Airfoil with Bilinear and Cubic Structural Nonlinearities," *Journal of Fluids and Structures*, **9**, pp. 175-193 (1995).
2. Poirel, D. C. and Price, S. J., "Post-Instability Behavior of a Structurally Nonlinear Airfoil in Longitudinal Turbulence," *Journal of Aircraft*, **34**, pp. 619-627 (1997).
3. Lee, B. H. K., Price, S. J. and Wong, Y. S., "Nonlinear Aeroelastic Analysis of Airfoils: Bifurcation and Chaos," *Progress in Aerospace Sciences*, **35**, pp. 205-334 (1999).
4. Poirel, D. C. and Price, S. J., "Structurally Nonlinear Fluttering Airfoil in Turbulent Flow [J]," *AIAA Journal*, **39**, pp. 1960-1968 (2001).
5. Poirel, D. and Price, S. J., "Response Probability Structure of a Structurally Nonlinear Fluttering Airfoil in Turbulent Flow," *Probabilistic Engineering Mechanics*, **18**, pp. 185-202 (2003).
6. Poirel, D. and Price, S. J., "Bifurcation Characteristics of a Two-Dimensional Structurally Non-Linear Airfoil in Turbulent Flow," *Nonlinear Dynamics*, **48**, pp. 423-435 (2007).
7. Poirel, D., Harris, Y. and Benaissa, A., "Self-Sustained Aeroelastic Oscillations of a NACA0012 Airfoil at Low-to-Moderate Reynolds Numbers," *Journal of Fluids and Structures*, **24**, pp. 700-719 (2008).
8. Poirel, D. and Yuan, W., "Aerodynamics of Laminar Separation Flutter at a Transitional Reynolds Number," *Journal of Fluids and Structures*, **26**, pp. 1174-1194 (2010).
9. Poirel, D. and Mendes, F., "Experimental Small-Amplitude Self-Sustained Pitch – Heave Oscillations at Transitional Reynolds Numbers [J]," *AIAA Journal*, **52**, pp. 1581-1590 (2014).
10. Yuan, W., Poirel, D. and Wang, B., "Simulations of Pitch – Heave Limit-Cycle Oscillations at a Transitional Reynolds Number," *AIAA Journal*, **51**, pp. 1716-1732 (2013).
11. Huang, Y., Fang, C. and Liu, X., "On Stochastic Dynamical Behaviors of Binary Airfoil with Nonlin

https://doi.org/10.1017/jmech.2018.19 Published online by Cambridge University Press

Ear Structure," *Acta Aeronautica et Astronautica Sinica*, **31**, pp. 1946-1952 (2010).

12. Zhao, D. M., Zhang, Q. C. and Tan, Y., "Random Flutter of a 2-DOF Nonlinear Airfoil in Pitch and Plunge with Freeplay in Pitch," *Nonlinear Dynamics*, **58**, pp. 643-654 (2009).
13. Yang, Z. C. and Zhao, L. C., "Analysis of Limit Cycle Flutter of an Airfoil in Incompressible Flow," *Journal of Sound and Vibration*, **123**, pp. 1-13 (1988).
14. Berggren, D., "Investigation of Limit Cycle Oscillations for a Wing Section with Nonlinear Stiffnes," *Aerospace Science and Technology*, **8**, pp. 27-34 (2004).
15. Chassaing, J. C., Lucor, D. and Gon, J. T., "Stochastic Nonlinear Aeroelastic Analysis of Asupersonic Lifting Surface Using an Adaptive Spectual Method," *Journal of Sound and Vibration*, **331**, pp. 394-411 (2012).
16. Dowell, E. H., Thomas, J. P. and Hall, K. C., "Transonic Limit Cycle Oscillation Analysis Using Reduced Order Aerodynamic Models," *Journal of Fluids and Structures*, **19**, pp. 17-27 (2004).
17. Christiansen, L. E. *et al.*, "Nonlinear Characteristics of Randomly Excited Transonic Flutter," **58**, pp. 385-405 (2002).
18. Missoum, S., Dribusch, C. and Beran, P., "Reliability-Based Design Optimization of Nonlinear Aeroelasticity Problems," *Journal of Aircraft*, **47**, pp. 992-998 (2010).
19. Dribush, C., "Multi-Fidelity Construction of Explicit Boundaries: Application to Aeroelasticity," *University of Arizone*, 2013.
20. Dribusch, C., Missoum, S. and Beran, P., "A Multifidelity Approach for the Construction of Explicit Decision Boundaries: Application to Aeroelasticity," **42**, pp. 693-705 (2010).
21. Dimitriadis, G. and Li, J., "Bifurcation Behavior of Airfoil Undergoing Stall Flutter Oscillations in Low-Speed Wind Tunnel," *AIAA Journal*, **47**, pp. 2577-2596 (2009).
22. Wu, Z. Q. and Zhang, J. W., "Complicated Bifurcations In Limit-Cycle Flutter Of Two-Dimensional Airfoil," *Engineering Mechanics*, **25**, pp. 52-55 (2008).
23. Wang, H. L. and Wu, Z. Q., "Nonlinear Vibration of the High Dimensional Systems with Parameters," *Acta Mechanica Sinica*, **28**, pp. 109-113 (1996).
24. Hao, Y. and Wu, Z. Q., "Stochastic P-Bifurcation of Tri-Stable Van der Pol-Duffing Osciliator," *Acta Mechanica Sinica*, **45**, pp. 257-265 (2013).
25. Wu, Z. Q. and Hao, Y., "Three-Peak P-Bifurcation in Stochastically Excited Van der Pol-Duffing Oscillator," *Scientia Sinica Physica, Mechanica & Astronlmica*, **4**, pp. 524-529 (2013).
26. Zakharova, A. *et al.*, "Stochastic Bifurcations and Coherencelike Resonance in a Self-Sustained Bistable Noisy Oscillator," *Physical Review E*, **81**, (2010).

(Manuscript received November 9, 2017,
accepted for publication March 27, 2018.)

https://doi.org/10.1017/jmech.2018.19 Published online by Cambridge University Press